symmetry

MDPI

Article

Modern Dimensional Analysis-Based Steel Column Heat Transfer Evaluation Using Multiple Experiments

Renáta-Ildikó Száva [1], Ioan Száva [1,*], Sorin Vlase [1,2,*], Pál-Botond Gálfi [1], Károly Jármai [3], Teofil Gălățeanu [1], Gabriel Popa [1] and Zsolt Asztalos [1]

1 Department of Mechanical Engineering, Transilvania University of Brasov, B-dul Eroilor, 29, 500036 Brasov, Romania
2 Romanian Academy of Technical Sciences, Bulevardul Dacia 26, 030167 Bucharest, Romania
3 Department of Mechanics, University of Miskolc, 3529 Miskolc, Hungary
* Correspondence: eet@unitbv.ro (I.S.); svlase@unitbv.ro (S.V.)

Abstract: In order to foresee the response during the fire of a real symmetrical structure (prototype), nowadays engineers apply methods which involve the associated reduced-scale model's behaviors, mainly dimensional analysis behaviors. Between the dimensional analysis methods, the so-called Modern Dimensional Analysis (*MDA*), developed by Szirtes, fulfills all engineering requirements compared with the classical one. The authors used this new proposed method to describe their original electric fire simulation testing bench, as well as the Model Law (using *MDA*) for the heat transfer in tubular rectangular bars. So, a validation of the Model Law was performed based on several scrupulous experimental investigations both on a real column's segment and its associated reduced-scale models manufactured at 1:2; 1:4, as well as 1:10 scales. The original heating system, the elaborated protocol, the deduced Model Law, and the results of the experimental investigations represent the contributions of the authors in the field of metallic structures subject to fires. The results validate the possibility of using *MDA* in the case of heat transmission.

Keywords: modern dimensional analysis (*MDA*); model law (*ML*); steel column; scale models; heat transfer; multiple experiments

check for updates

Citation: Száva, R.-I.; Száva, I.; Vlase, S.; Gálfi, P.-B.; Jármai, K.; Gălățeanu, T.; Popa, G.; Asztalos, Z. Modern Dimensional Analysis-Based Steel Column Heat Transfer Evaluation Using Multiple Experiments. *Symmetry* **2022**, *14*, 1952. https://doi.org/10.3390/sym14091952

Academic Editors: Jan Awrejcewicz and Sergei D. Odintsov

Received: 31 July 2022
Accepted: 14 September 2022
Published: 19 September 2022

Publisher's Note: MDPI stays neutral with regard to jurisdictional claims in published maps and institutional affiliations.

Copyright: © 2022 by the authors. Licensee MDPI, Basel, Switzerland. This article is an open access article distributed under the terms and conditions of the Creative Commons Attribution (CC BY) license (https://creativecommons.org/licenses/by/4.0/).

1. Introduction

The issue of the fire resistance of structural elements depends to a large extent on [1] their quality (usually steels); their protection against the propagation of heat; and how this process can be theoretically simulated and experimentally verified. Regarding protection methods, especially with the help of thermal foam paints, called intumescents, a series of effective solutions are offered in reference [2]. In reference [3], the author offered useful protocol of fire tests in order to establish the cellular beam behaviors foreseen with an intumescent paint layer. The problem of fire resistance, in general, as well as the theoretical approach to the fire resistance of these structural elements can be found, among others, in reference [4], but the specialized literature obviously offers an even wider range of approaches, such as reference [5], respectively [6]. Based on reference [7], one can obtain a real insight on the state-of-the-art of thermal insulation materials, and reference [8] offered the main aspect of the fire phenomena as well as its classical theoretical approach, too. In reference [9], the authors analyzed some very widely used temperature protection classes of materials, applied in fire-protection problems. The authors of reference [10] offered a very useful sensitivity analysis on heat-transfer formulation in thermal insulated steel structural elements. In reference [11], the authors presented results obtained by experimental investigations in the local buckling problems of steel members subjected to fire. High-accuracy numerical simulation, performed by the authors of reference [12], had as its goal the analysis of structural elements with cross-sections characterized by high-value shape factors, i.e., tubular cross-sections such as I and U profiles. The authors of reference [13]

described a comparison of Eurocod 3 and the NIST (National Institute of Standards and Technology, Gaithersburg, MD, USA) models regarding the high-temperature stress–strain correlation based on high-accuracy experimental investigations. In order to compare the critical buckling temperatures with the experimental data, as well as to evaluate the temperature variation along the structural elements, the authors performed meticulous Finite Elements studies, with/having a closer fitting (less than 1%) with the experiments than the Eurocode 3. In reference [14], the authors performed both numerical simulation and experimental tests in order to verify that even the concrete–steel composite beams have a better fire resistance as compared with the common steel ones. In the experimental investigations, as a fire-protection material, they used a fireproof spray coating applied in the same thickness. The structural members were subjected to the standard fire conditions. They found some useful correlations between the shape factor, the temperature increase, and the fire resistance of the structural elements. In order to predict the structural behaviors under real fire conditions, the authors of reference [15] developed a combined Fire-Dynamics Simulator and Finite Element Method, taking into the consideration the previously obtained results at NIST, USA. The validation of the mentioned method, using real-scale structural elements tests, was successful, and had minimal error, e.g., the final buckling time was predicted with less than 10% of the experimentally obtained one. In reference [16], the authors performed several experimental studies on the temperature distribution of T-,Y-, K-, and KT-types of joints, applied in SHS (Square Hollow Section) structural elements joining; a standard ISO-834 fire condition was applied, without mechanical loading, on several unprotected welded SHS specimens. They found that the temperature distribution around the joint was significantly influenced by the dimension of the brace cross-section and β, which is the brace/chord diameter ratio. In the reference [17], the fire resistance at SHS and the CHS (Circular Hollow Section) structural members manufactured at full-scale with different types of joints was studied. The standard fire condition as well as an axial loading represented the experimental conditions. In a similar manner, in reference [18] the authors performed a parametric study on some circular tubular K-joints subjected to high temperatures. Several investigations on the fire resistance of tubular K-joints, based on the critical temperature method, were performed by the authors of reference [19]. The authors of reference [20] performed similar investigations. In reference [21], a comparative Finite Element (ABAQUS), analytical calculus based on Euro-code 3 and experimental investigations was performed on the heat transfer problem of tubular steel columns under standard fire test (ISO 834). The columns were subjected not only to the fire action but also to different axial loadings. Based on the obtained results, they concluded that this heat transfer law is not influenced by the loading type and its magnitude, but the shape factor of the cross-section influences the value of the critical temperature. In reference [22], the effect of the localized fire in a building's compartments on the load-bearing capacity of the full-scale CHS steel columns, together with the corresponding thermal distribution laws, was investigated. The influences of different ambient parameters were also taken into consideration. In reference [23], a meticulous analytical temperature evaluation of a four-side heated column's (at standard fire) temperature distribution was performed, taking into consideration different Euro-codes. In reference [24], the authors offered an analytical heat transfer model for unprotected steel members subjected to standard fire in a closed compartment. The obtained results are useful for the unprotected *I*-steel columns, offering better results than those based on the Stefan–Boltzmann relation, which presumes a constant emissivity. Compared with the studies mentioned above, the authors of the present contribution started with detailed experiments on reduced-scale structural elements, as described in the following sections.

Another important aspect consists of the modeling of the processes that take place during a fire [25], respectively, and the propagation of the thermal flow introduced into them during the development of the fire.

Taking the significance of the fire protection, as well as its evaluation based on reduced-scale elements instead of the real structural elements into consideration, several approaches

over time have used, in this sense, Geometric Analogy and Similarity Theory [26], respectively, in the case of complex phenomena, such as this one of fire resistance: Classical Dimensional Analysis (*CDA*). Due to the fact that during the last century the *CDA* literature was increasing day by day, nowadays, the literature is plentiful and one can mention, without putting in evidence their particularities, some of the most well-known books and scientific papers, mentioned in references such as [27–45], in order to offer to readers some significant references. Neither the present journal nor this paper had as their goal the step-by-step analysis and evaluation concerning their advantages as well as their limits.

Unfortunately, all these previously mentioned methods present a series of shortcomings, which the authors have analyzed in detail in references [1,46], which is why their applicability by the broad mass of researchers is usually difficult. *CDA* is not exempt from these shortcomings either, although at first glance it offers a wide range of opportunities. As is well known, *CDA* uses, as the Similarity Theory, a set of dimensionless variables $\pi_j,\ j = 1,\ \ldots\ n$ based on which the so-called Model Law (*ML*), which describes/governs the behavior of the prototype based on the experimental data obtained from the attached model (usually made on a small scale).

Thus, the data of experimental investigations from the model, through the elements of the *ML* (in number of $j = 1,\ \ldots\ n$), will predict the behavior of the prototype in real operating conditions.

For this reason, *CDA* is not an easy method for the average researcher, as it is usually left to established specialists. Against this, Szirtes developed a unitary, simple, and particularly accessible methodology for any researcher, hereinafter referred to as Modern Dimensional Analysis (*MDA*), synthesized in his works [41,42].

As was mentioned before, the authors of this paper applied the principles of *MDA* in solving some problems in different fields of engineering, including that of civil engineering, but also in that of heat transfer, which is the starting point in the analysis of resistance to fire of structural elements.

Within these works, there are critical evaluations of the previously mentioned methods, but also the net advantages of *MDA*, which are illustrated by concrete examples. In reference [40], applying the principles of *MDA*, the authors deduced for the general case of a rectangular–tubular-section steel bar the Model Law, which governs the heat transfer.

In reference [40], the method of obtaining the 50 dimensionless variables involved, as well as how the Model Law resulted from, this set of dimensionless variables, 50 elements, was presented. Of these, according to reference [40], some were dedicated/destined to experimental investigations, others to theoretical investigations, and others to those classical similitude criteria also reported in specialized works (Re, Nu, Bi, etc.), which can be obtained and based on *CDA*. Of these, those related to experimental investigations were of major interest and easy to verify/validate, and the authors chose from these those represented by relations (1) and (2) for variant I, respectively, (3) and (4) for variant II.

We can mention the fact that the vast majority of the dimensionless variables determined with the help of *MDA*, respectively, the elements of the Model Law deduced by the authors, cannot be obtained with the help of *CDA* or other classical methods of approach (Geometric Analogy or Similitude Theory) in the case of against-thermal transfer, except for those similarity criteria mentioned above which are considered classical (Re, Nu, Bi, etc.).

The methodology is particularly simple, unitary, and flexible; this flexibility is manifested, among others, by the possibility of choosing different materials for the prototype and the model, but also other facilities, illustrated in references [41,42], as well as in the previous ones of the authors [39,40,43–45], which governs the heat transfer. In reference [46], the authors performed the validation of these laws for the specific case of some sets of structural elements made at scales 1:1, 1:2, and 1:4 (Figure 1).

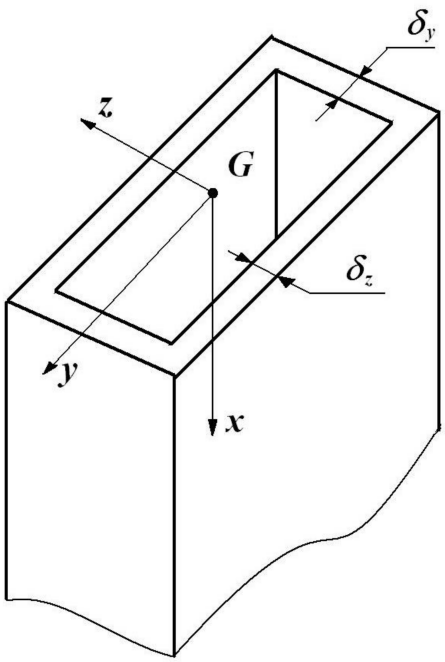

Figure 1. Beam with a rectangular-hole section [40].

In this paper, the authors presented the results of their experimental investigations regarding the extension of the applicability of these laws of the model to structural elements made at a scale of 1:10.

In this sense, it is worth summarizing the indisputable advantages of *MDA* presented in the paper, namely:

- *MDA* does not require deep knowledge in the field, only the review of the variables (along with their dimensions), which can, to a certain extent, influence the analyzed phenomenon;
- the unitary protocol of the *MDA* allows the automatic elimination of variables with insignificant/irrelevant influence (either from the physical point of view or from the magnitude point of view), without the researcher having any other algorithm to apply;
- *MDA* provides, in all cases, the complete set of dimensionless variables and therefore of the *ML*, which the rest of the methods cannot provide, except in very special cases;
- from this complete set, by eliminating some variables, which are identical to the prototype and the model, one can formulate/obtain the particular sets related to simpler cases.

The studied case presented in this paper and the results of the experimental test highlight the relevance and the advantage of using this method in this new field of application.

2. Materials and Models

From reference [40], where the complete set of the *ML* was deduced for two practically significant versions, the following relevant elements were retained, namely for the following:

- Version I, where the set of independent variables was $(Q,\ L_z\ ,\ \Delta t,\ \tau,\ \lambda_{x\ steel},\ \varsigma)$, was chosen:

$$S_{\dot{Q}} = \frac{S_Q}{S_\tau}, \tag{1}$$

$$S_{A_{tr}} = \frac{S_{L_z}}{S_\varsigma}, \tag{2}$$

- Version II, where the set of independent variables was $(Q,\ L_z\ ,\ \Delta t,\ \tau,\ \lambda_{x\ steel},\ \varsigma)$, was chosen:

$$S_Q = S_{\dot{Q}} \cdot S_\tau, \tag{3}$$

$$S_{A_{tr}} = \frac{S_{L_z}}{S_\varsigma}, \tag{4}$$

where: $Q\ (J)$ represents the invested heat; $\dot{Q}\ (W)$—the heat rate; $L_z(m)$—the beam dimension along direction z; $\Delta t\ (^\circ C)$—the temperature variation; $\tau\ (s)$—the time; $\lambda_{x\ steel}\ (\frac{W}{^\circ C \cdot m})$—the thermal conductivity; $\varsigma = \frac{P}{A}\ (\frac{1}{m})$—the shape factor; $P\ (m)$—the perimeter of the cross-section; $A\ (m^2)$—the area of the cross-section; $S_\omega = \frac{\omega_2}{\omega_1}\ (-)$—the scale factor of the variable ω, with index "1" for prototype, respectively with "2" for the model.

Remarks:

- The case of the quadratic section represents a particular case of the rectangular one, where on the two directions y and z there exist the same dimensions and the same scale factors;
- If it is desired, however, that the scale factors of the dimensions along the z and y directions have different values, respectively, one should admit different thicknesses in the two directions, and then one will have $(S_{L_x} \neq S_{L_y} \neq S_{L_z} \neq S_{\delta_{y,\ steel}} \neq S_{\delta_{z,\ steel}})$ and correspondingly these elements/variables for the model will be rigorously obtained only from the *ML*;
- Taking into account that length L_z is considered an independent variable, and thus freely chosen a priori, for both the prototype and model, the Model Law elements for the rest of the dimensions $\left(L_x\ ,\ \ L_y\ ,\ \ \delta_{y\ steel}\ ,\ \ \delta_{z\ steel}\right)$ can be ignored, each having the same scale factor of lengths S_L, which is why it makes no sense to analyze them and their validity;
- The advantage of including the shape factor ς in the set of independent variables, in addition to that of the length L_z, resides in the fact that one will be free of the restriction of a geometric similarity of the cross-sections of the prototype and the model (so, let us have, for example, only rectangular sections), allowing one to accept a section of another shape in the model, only to respect the initially established scale factor.

It can be noted that, in both cases, the set of independent variables was rigorously related to the actual measurements. In the latter, the value for the model was chosen in advance (before starting the experiments), and based on the measurement results, the desired value for the prototype results from the *ML*. In the case of Version I, it is the heat flow $\dot{Q}$, while in the case of Version II, this is the amount of heat Q.

The authors, starting from the case of an existing pillar used in constructions made at 1:1, 1:2, and 1:4 scales, respectively, a 1:10 scale prototype as well as the related models. Consequently, 6 sets of prototype models could be identified, that is, (1:1–1:2); (1:1–1:4); (1:1–1:10); (1:2–1:4); (1:2–1:10); and (1:4–1:10), which were not protected with intumescent paint. They applied identical thermal regimes to all these structural elements and recorded all parameters related to these thermal regimes. The above-mentioned quantities obtained by rigorous direct measurements (on the elements considered as models) were compared with those resulting by applying the *ML* for those taken as prototypes, obtaining a very good correlation, which proves the validity of these laws for practically any structure carried out on a desired scale. Consequently, these laws will allow obtaining very convenient models from the point of view of experimental simulations for complex structures (for example, industrial halls with several compartments, respective floors, having one or more fire foci arranged/located on the structure as desired). The measurement data obtained on these models, i.e., their responses to fires, will serve, by applying these *ML*, to optimize real structures subjected to similar fires.

The original stand used in their heating/testing, together with the electronic command and control system, as well as data acquisition, were presented in references [1,45], and are succinctly summarized below.

In Figure 2 and Table 1, according to references [45,46], the dimensions of these structural elements subjected to tests are presented. The upper closing plate with the dimensions (axb)

serves to replace the rest of the column; the lower one, with the unique dimensions (mxn), serves to ensure a perfect and uniform placement of all the elements tested on the test stand (a central hole with a diameter of 0.005 m being provided to allow the air to escape during the heating of the respective structural element and thus eliminate the risk of unwanted deformations thereof). Figure 3 shows the assembly of the original stand, where the structural element *1* will sit on the dome in the form of a pyramidal trunk *2*, which in turn rests on the rigid frame *3* and the supporting legs *4*. In section A-A. the heating elements *6* are shown, consisting of twelve Silite rods (connected four in series for the three phases of the industrial supply current at 380 V). Silite bars are placed on the fireclay bricks *7*, under which there is a heat-insulating blanket *8* made of ceramic fiber with a thickness of 0.0254 m. A similar insulation *5* is also provided for the side walls of the pyramid trunk *2*. During the experimental investigations, the free surface of the laying plate, with the dimensions (mxn) shown in Figure 2, is covered with such a heat-insulating blanket.

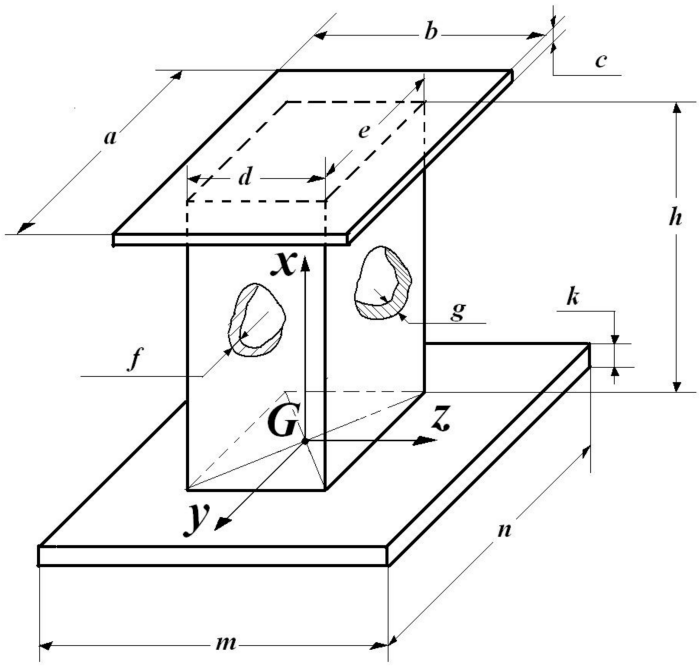

Figure 2. Dimensions of the tested specimens [1]. *Gx, Gy, Gz* represent the axis of the coordinate system and the other letter represent the dimensions of the test specimen.

Table 1. Dimensions of the tested specimens [40].

	Dimensions, in *m* for Element at Scale			
	1:1	1:2	1:4	1:10
a	0.370	0.185	0.108	0.0370
b	0.370	0.185	0.108	0.0370
c	0.006	0.003	0.0015	0.0015
d	0.350	0.175	0.0875	0.0030
e	0.350	0.175	0.0875	0.0030
f	0.016	0.008	0.004	0.0015
g	0.016	0.008	0.004	0.0015
h	0.400	0.200	0.100	0.400
k	0.010	0.005	0.0025	0.0015
m	0.450	0.450	0.450	0.450
n	0.450	0.450	0.450	0.450

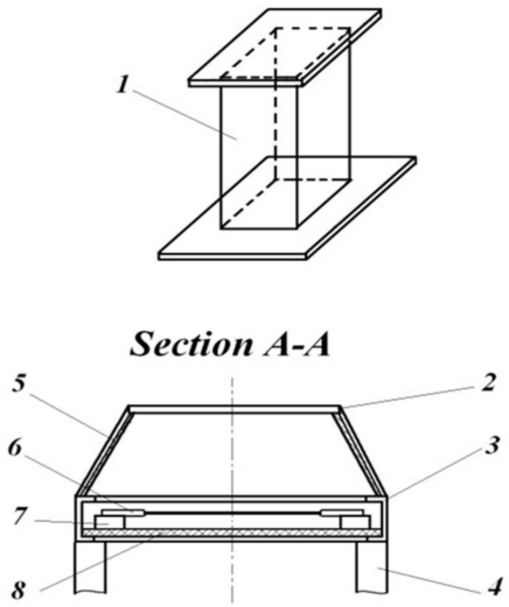

Figure 3. Test stand [1]: structural element *1*, pyramidal trunk *2*, rigid frame *3*, supporting legs *4*, insulation blanket *5*; heating elements *6*, fireclay bricks *7*, heat-insulating blanket *8*.

As an illustration of the degree of thermal insulation, it can be mentioned that, at the nominal heating temperature $t_{o,\ nom} = 600\ ^{\circ}C$ of the structural elements subjected to tests, around the support frame *3* and the pyramid trunk *2*, the temperature did not exceed $(45\ \ldots\ 50)\ ^{\circ}C$, which obviously had much lower values at temperatures up to $t_{o,\ nom} = 500\ ^{\circ}C$.

To emphasize the efficiency of this original electronic control and regulation system, briefly presented in reference [46], it ensures optimal operation in a wide range of dissipated power, as well as precise monitoring of the electrical energy consumed for heating. Thus, at the nominal value of the supply voltage, the heating system provides a power of approx. 25 kW, as well as reaching temperatures $t_{o,\ nom} = (500\ \ldots\ 600)^{\circ}C$ from the base of the structural element under test, so it can be mounted and used in relatively modestly equipped laboratories.

In Table 2, according to references [1,45,46], the fixing positions of PT 100-402-type thermoresistances, with 0.150 m-long terminals and with a measurement range between $(-70\ \ldots\ +500\ ^{\circ}C)$, in relation to the reference system $xGyz$ are presented (Figure 2). At each level, four thermoresistances were fixed by means of M3 screws (one in the middle of each side), and the arithmetic mean of their indications constituted the temperature of the column segment at that level.

Table 2. Co-ordinates $x(j)$, m of the mounted PT-100′s.

At Scale 1:1	At Scale 1:2	At Scale 1:4	At Scale 1:10
0.020	0.020	0.020	0.015
0.110	0.060	0.055	0.030
0.200	0.105	0.090	0.045
0.290	0.150		0.060
0.380	0.190		0.100
			0.200
			0.400
			0.460
			0.495

It seems (at first sight) that an excessively large number of thermoresistors would have been fixed on the structural element made at the 1:10 scale, but it models the pole as a whole. In the case of a whole column (not the column segment as in the first three structural elements) where, based on the reasoning detailed in references [1,2], as well as taking into account the authors' detailed experimental research [40] on rectangular-tubular structural elements, it was possible to demonstrate that, compared with the full circular section, a single exponential law describes the heat flow propagation, here, at the tubular ones, at least three intervals with distinct exponential laws must be taken into account, i.e., on $z_I \in [0 \div 6] \cdot L[\%]$; $z_{II} \in [6 \div 12] \cdot L\ [\%]$; and $z_{III} \in [12 \div 100] \cdot L[\%]$. Consequently, in the present case, this division led to $z_I \in [0 \div 0.03](m)$; $z_{II} \in [0.03 \div 0.06](m)$; $z_{III} \in [0.06 \div 0.50]\ (m)$, thus making it possible to accurately approximate these initial (theoretical) exponential curves by polynomial functions of relatively low degrees [1,2].

As previously mentioned, all the structural elements were rigorously subjected to identical thermal regimes reaching the same nominal temperatures $t_{o,\ nom}(^\circ C)$, so the scale factor of the temperatures being the same $S_{\Delta\ t} = \frac{\Delta t_2}{\Delta t_1} = ct = 1$ no longer appeared in the above-mentioned elements of the *ML*, obtaining the simplified relations from relations (1)–(4).

The experimental measurement protocol was as follows:

- mounting the stand, with the provision of rigorous thermal insulation with the help of suitable special mattresses (Figure 3);
- mounting, on the lower plate with the dimensions (mxn) of the tested structural element, a thermocouple type K (intended to control the nominal temperature $t_{0,\ nom}$), as well as all thermoresistances type PT 100-402 at the elevation level $x(j)$, according to Table 2;
- connecting the thermoresistances to the data acquisition system;
- checking the proper functioning of all elements;
- selection of nominal temperature $t_{0,\ nom}$;
- selection of the steps of the heating regime;
- connecting the stand to the 380 V power source;
- starting the installation and monitoring the reaching of the temperature $t_{0,\ nom}$;
- recording the electrical energy consumed $E_{0,total}\ [kWh]$, as well as the time $\tau_{0,total}\ [s]$ required to reach this stabilized thermal regime;
- resumption of stages to reach all nominal temperatures of $t_{0,\ nom} = (100,\ 200,\ 300,\ 400,\ 450,\ 500)\ ^\circ C$.

Remarks:

- The control electronic temperature system also has a self-learning function; so, basically, after the first cycle of reaching the nominal temperature $t_{0,\ nom}$, it will ensure the temperature control within very limited limits. For example, at $t_{0,\ nom} = 500\ ^\circ C$, the thermal oscillations related to the regulation were at maximum $(4\ \ldots\ 5)\ ^\circ C$;
- The achievement of a stabilized temperature regime was considered to be achieved; when at the level of the last thermoresistance PT 100-402 (near the upper part of the tested structural element) the maximum temperature oscillations $(0.2\ \ldots\ 0.3)\ ^\circ C$ were observed for a period of minimum $(120\ \ldots\ 180)\ s$.

After reaching this stabilized regime, the total amount of electrical energy invested in the system without energy loss $E_{0,total}\ [kWh]$ from the beginning of the heating process corresponds to a total amount of heat invested at the level of the stand:

$$Q_{0,total}\ [J] = E_{0,\ total}[kWh] \cdot 3.6 \cdot 10^6, \tag{5}$$

because $1\ kWh = 3600\ kWs = 3600\ kJ = 3.6 \cdot 10^6\ J$.

The total heat losses through the thermal insulation blankets were determined with the relation:

$$Q_{waste,\ total} = Q_{w,\ total} = \sum [\lambda \cdot \Delta t \cdot \Delta\tau \cdot (\sum \frac{A_k}{h_k})], \tag{6}$$

where: $\lambda\ (\frac{W}{m \cdot K} = \frac{W}{m \cdot {}^{\circ}C})$ is the thermal conductivity coefficient of the thermal insulation blanket, which, based on the manufacturer's recommendation for the material used, depending on the temperature $t^{\circ}C$ reached on its heated side, had the calculation relationship:

$$\lambda\ (\frac{W}{m \cdot {}^{\circ}C}) = 0.0002 \cdot t\ ({}^{\circ}C) + 0.03, \tag{7}$$

$\Delta t\ ({}^{\circ}C)$—temperature difference reached during heating;
$\Delta\tau\ (s)$—the time required to reach it;
$A_k\ (m^2)$—the unfolded areas of the k heat-insulating blankets applied around the stand, having the thickness $h_k\ (m)$.

Additionally, taking into account the peculiarity of the heating system through the thermoregulation presented before, because instead of a linear law of temperature increase from $t_B \equiv t_i$ to $t_D \equiv t_n$ (shown with the broken line in Figure 4), from the actual acquisition of the data a funicular polygon resulted $(B \equiv i - j - k - l - m - n \equiv D)$, in which the relations (5) and (6) should be adapted as follows:

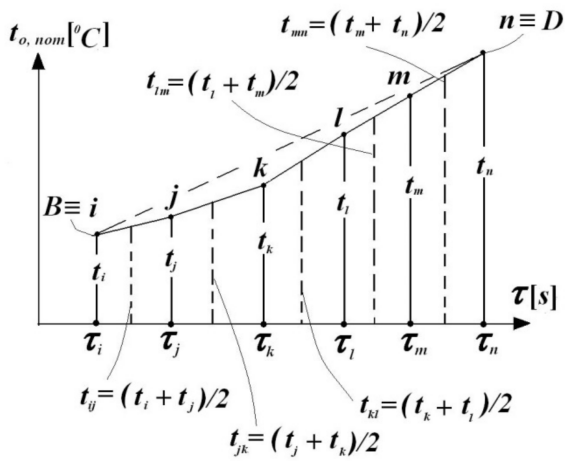

Figure 4. Particularity of the stand heating [1].

- in relation (5), for each interval $(i-j)$; $(j-k)$; $(k-l)$; $(l-m)$; $(m-n)$, the corresponding temperature difference ($\Delta t_{ij} = (t_j - t_i)$; $\Delta t_{jk} = (t_k - t_j)$; $\Delta t_{kl} = (t_l - t_k)$; $\Delta t_{mn} = (t_n - t_m)$) will be considered and applied to the $\Delta\tau$ time intervals corresponding to $\Delta\tau_{ij} = (\tau_j - \tau_i)$; $\Delta\tau_{jk} = (\tau_k - \tau_j)$; $\Delta\tau_{kl} = (\tau_l - \tau_k)$; $\Delta\tau_{lm} = (\tau_m - \tau_l)$; $\Delta\tau_{mn} = (\tau_n - \tau_m)$;
- λ the temperature differences are determined with relation (6) individually for each interval before, considering the average temperature related to each interval, respectively;
- the term $\sum \frac{A_k}{h_k}$, being constant, will multiply the sum of the partial products related to these intervals.

The total amount of heat invested for heating the structural element $Q_{total}(J)$ was obtained as the difference of the previous ones, i.e.,

$$Q_{total}[J] = Q_{0,\ total} - Q_{w,total}, \tag{8}$$

Considering the fact that the thermal radiation of the Silite bars only directly reached the lower support plate of the structural element in a proportion of 47.22%, corresponding to the angle $(2 \cdot 85^{\circ})$ from the total of 360° (Figure 5), then the amount of effective heat invested in the system can also be defined, i.e.,:

$$Q_{eff}[J] = Q_{0,\ eff} - Q_{w,\ total} = 0.4722 \cdot Q_{0,total} - Q_{w,\ total}, \tag{9}$$

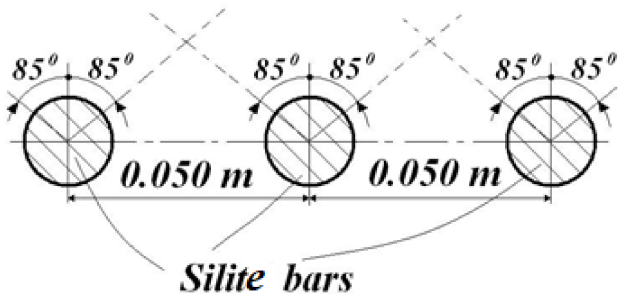

Figure 5. Effective heat transfer from the Silite bars [1].

It should be mentioned that the *ML* was verified (and duly validated) for this last particularization as well. The corresponding heat fluxes were determined based on the definition relation:

$$\dot{Q}\,(\frac{J}{s} = W) = \frac{dQ}{d\tau} = \frac{\Delta Q}{\Delta \tau}, \tag{10}$$

It is obvious that the amounts of heat, thermal flows, and the times required to reach higher thermal regimes were determined by summing the last values with those previously obtained.

Thus, for example, the parameters related to reaching the stabilized regime at $t_{0,\,nom} = 200\ ^{\circ}C$ resulted from summing the values obtained for the stabilized regime from $t_{0,\,nom} = 100\ ^{\circ}C$ with those obtained during the heating of the system in the temperature range $(100\ \ldots\ 200)\ ^{\circ}C$.

3. Results and Discussion

Based on the measurement data in Tables 3 and 4, these preliminary calculations are summarized.

Table 3. Preliminary calculus—Part I.Measured and Computed Values.

Structural Element	$\Delta t\ [^{\circ}C]$	$\varsigma\left[\frac{1}{m_y}\right]$	$E_{0,\,total}$ KWh	$Q_{0,\,total}\ [J]$	Δt_{total} $[^{0}C]$	$\sum \frac{A_k}{h_k}\ [m]$	$Q_{w,total}\ [J]$	$Q_{total}\ [J]$
At scale 1:10	23–100	0.7017543	0.5	1,800,000	77	20.34095	15,231.3	1,784,769
	100–200	0.7017543	0.8	2,880,000	100	20.34095	19,155.56	2,860,844
	200–300	0.7017543	1.4	5,040,000	100	20.34095	19,155.56	5,020,844
	300–400	0.7017543	2.1	7,560,000	100	20.34095	28,088.82	7,531,911
	400–450	0.7017543	0.8	2,880,000	50	20.34095	18,910.72	2,861,089
	450–500	0.7017543	0.5	1,800,000	50	20.34095	7799.208	1,792,201
At scale 1:4	23–100	0.2619760	0.4	1,440,000	77	20.07323	84,810.39	1,355,189.6
	100–200	0.2619760	0.6	2,160,000	100	20.07323	185,272.3	1,974,727.7
	200–300	0.2619760	1.4	5,040,000	100	20.07323	1,000,576	4,039,424
	300–400	0.2619760	1.4	5,040,000	100	20.07323	1,018,576	4,021,424.3
	400–450	0.2619760	2.9	1,0440,000	50	20.07323	2,709,526	7,730,474.3
	450–500	0.2619760	0.7	2,520,000	50	20.07323	572,461.5	1,947,538.5
At scale 1:2	23–100	0.1309880	0.6	2,160,000	77	19.17165	32,233.53	2,127,766.5
	100–200	0.1309880	1.1	3,960,000	100	19.17165	324,889.8	3,635,110.2
	200–300	0.1309880	0.8	2,880,000	100	19.17165	244,466.6	2,635,533.4
	300–400	0.1309880	1.3	4,680,000	100	19.17165	619,849.7	4,060,150.3
	400–450	0.1309880	0.8	2,880,000	50	19.17165	389,373	2,490,627
	450–500	0.1309880	1.2	4,320,000	50	19.17165	667,908.9	3,652,091.1
At scale 1:1	23–100	0.0654940	0.9	3,240,000	77	15.55354	41,696.8	3,198,303.2
	100–200	0.0654940	1.4	5,040,000	100	15.55354	323,210	4,716,790
	200–300	0.0654940	2.3	8,280,000	100	15.55354	391,377.5	7,888,622.5
	300–400	0.0654940	2.8	10,080,000	100	15.55354	510,624.9	9,569,375.1
	400–450	0.0654940	1.6	5,760,000	50	15.55354	459,366.7	5,300,633.3
	450–500	0.0654940	2.7	9,720,000	50	15.55354	777,565.4	8,942,434.6

Table 4. Preliminary calculus—Part II. Computed values of the variations.

Structural Element	Δt [°C]	$Q_{o,\,eff}$ [J]	Q_{eff} [J]	$\Delta\tau_{total}$ [s]	$\dot{Q}_{w,\,total}$ [J]	$\dot{Q}_{total}$ [W]	$\dot{Q}_{eff}$ [W]
At scale 1:10	23–100	849,960	834,728.7	2010	7.577763	887.9446	415.2879
	100–200	1,359,936	1,340,780	2790	6.865792	1025.392	480.5665
	200–300	2,379,888	2,360,732	3264	5.868738	1538.249	723.2636
	300–400	3,569,832	3,541,743	1926	14.58402	3910.65	1838.911
	400–450	1,359,936	1,341,025	1326	14.26148	2157.684	1011.331
	450–500	849,960	842,160.8	690	11.3032	2597.392	1220.523
At scale 1:4	23–100	679,968	595,157.6	2280	37.19754	594.3814	261.034
	100–200	1,019,952	834,679.7	1320	140.3578	1496.006	632.3331
	200–300	2,379,888	1,379,312	3000	333.5253	1346.475	459.7707
	300–400	2,379,888	1,361,312	1800	565.8754	2234.125	756.2846
	400–450	4,929,768	2,220,242	3600	752.646	2147.354	616.734
	450–500	1,189,944	617,482.5	660	867.3659	2950.816	935.5796
At scale 1:2	23–100	1,019,952	987,718.5	1260	25.58217	1688.704	783.9035
	100–200	1,869,912	1,545,022	2400	135.3708	1514.629	643.7592
	200–300	1,359,936	1,115,469	900	271.6296	2928.37	1239.41
	300–400	220,9896	1,590,046	1260	491.9442	3222.342	1261.942
	400–450	1,359,936	970,563	600	648.955	4151.045	1617.605
	450–500	2,039,904	1,371,995	840	795.1297	4347.727	1633.327
At scale 1:1	23–100	1,529,928	1,488,231	1860	22.41763	1719.518	800.1243
	100–200	2,379,888	2,056,678	2880	112.2257	1637.774	714.1243
	200–300	3,909,816	3,518,439	1560	250.883	5056.809	2255.409
	300–400	4,759,776	4,249,151	1200	425.5207	7974.479	3540.959
	400–450	2,719,872	2,260,505	780	588.9316	6795.684	2898.084
	450–500	4,589,784	3,812,219	1080	719.9679	8280.032	3529.832

In order to validate the Model Law in the two versions (I, respectively II), all of the calculations related to the significant variables involved were performed. In the case of version I, where the set of independent variables was $(Q,\ L_z\ ,\ \Delta t,\ \tau,\ \lambda_{x\ steel},\ \varsigma)$, heat flux remained the main dependent variable $\dot{Q}$, which had to be determined using the *ML* for the prototype (based on the measurements made on the model).

Similarly, in the case of version II, where the set of independent variables was $(\dot{Q},\ L_z\ ,\ \Delta t,\ \tau,\ \lambda_{x\ steel},\ \varsigma)$, the dependent variable sought for the prototype became the quantity of heat Q.

Obviously, in these experimental investigations, all the variables were known (being determined by actual measurements), but the problem consisted of finding the values of the dependent variables through the *ML* depending on the chosen option (version I or version II) precisely to be able to validate the *ML*.

In order to perform as rigorous an analysis as possible, the following prototype-model sets were considered, both for the unprotected and for the intumescent paint-protected versions:

- Prototype (structural element made at 1:1 scale) model (structural element made at 1:2 scale), symbolized by (1:2/1:1) Model/Prototype;
- Prototype (structural element made at 1:2 scale) model (structural element made at 1:4 scale), symbolized by (1:4/1:2) Model/Prototype;
- Prototype (structural element made at 1:1 scale) model (structural element made at 1:4 scale), symbolized by (1:4/1:1) Model/Prototype;
- Prototype (structural element made at 1:1 scale) model (structural element made at 1:10 scale), symbolized by (1:2/1:10) Model/Prototype;
- Prototype (structural element made at 1:2 scale) model (structural element made at 1:10 scale), symbolized by (1:4/1:10) Model/Prototype;
- Prototype (structural element made at 1:1 scale) model (structural element made at 1:10 scale), symbolized by (1:4/1:10) Model/Prototype;

Depending on the role of the structural element within a certain set, parts of the measurement data were considered as data acquired directly through measurements, and others served as reference values for those that should get them through *ML*.

Tables 5 and 6 summarize the results of these calculations for Version I and Tables 7 and 8 summarize those corresponding to Version II.

Table 5. Version I. Measured values.

		Measured Values			
Model/Prototype	**Tmin–Tmax Δt [°C]**	S_{ς} [−]	$S_{\Delta\tau_{total}}$ [−]	$S_{Q_{total}}$ [−]	$S_{Q_{eff}}$ [−]
	23–100	2	0.677419	0.66528	0.663686
	100–200	2	0.37037	0.809873	0.84502
1:2/1.0	200–300	2	0.576923	0.334093	0.317035
	300–400	2	1.05	0.424286	0.374203
	400–450	2	0.769231	0.469873	0.429357
	450–500	2	0.777778	0.4084	0.359894
	23–100	2	1.809524	0.636907	1.449594
	100–200	2	0.55	0.543237	0.540238
	200–300	2	3.333333	1.532678	1.236531
1:4/1:2	300–400	2	1.428571	0.990462	0.856146
	400–450	2	6	3.103827	2.287582
	450–500	2	0.785714	0.533267	0.450062
	23–100	4	1.225806	0.423721	0.400084
	100–200	4	0.203704	0.439953	0.456512
1:4/1.0	200–300	4	1.923077	0.512057	0.392024
	300–400	4	1.5	0.420239	0.320373
	400–450	4	4.615385	1.458406	0.982188
	450–500	4	0.611111	0.533267	0.161975
	23–100	10.71479	1.080645	0.558036	0.560886
	100–200	10.71479	0.430556	0.637373	0.733314
1:10/1.0	200–300	10.71479	2.092308	0.636467	0.67096
	300–400	10.71479	1.605	0.787085	0.833518
	400–450	10.71479	1.7	0.539764	0.593241
	450–500	10.71479	0.638889	0.200415	0.220911
	23–100	5.357394	1.595238	0.838799	0.845108
	100–200	5.357394	1.1625	0.787004	0.867807
1:10/1:2	200–300	5.357394	3.626667	1.905058	2.116358
	300–400	5.357394	1.528571	1.855082	2.227447
	400–450	5.357394	2.21	1.148743	1.381698
	450–500	5.357394	0.821429	0.490733	0.613822
	23–100	2.678697	0.881579	1.316736	1.401923
	100–200	2.678697	2.113636	1.448729	1.606341

Table 6. Version I. Computed values.

		Reference Values (Values for Validation)			Calculated Values with the *ML*		
Model/Prototype	**Tmin–Tmax Δt [°C]**	$S_{A_{tr}}$ [−]	$S_{\dot{Q}_{total}}$ [−]	$S_{\dot{Q}_{eff}}$ [−]	$S_{\dot{Q}_{total}}$ [−]	$S_{\dot{Q}_{eff}}$ [−]	$S_{A_{tr}}$ [−]
	23–100	0.25	0.98208	0.9797	0.9820	0.97972	0.25
	100–200	0.25	2.186656	2.2815	2.1866	2.28155	0.25
1:2/1.0	200–300	0.25	0.579094	0.5495	0.5790	0.54952	0.25
	300–400	0.25	0.404082	0.3563	0.4040	0.35638	0.25
	400–450	0.25	0.610836	0.5581	0.6108	0.55816	0.25
	450–500	0.25	0.525086	0.4627	0.5250	0.46272	0.25
	23–100	0.25	0.352042	0.3331	0.3520	0.80109	0.25
	100–200	0.25	0.987704	0.9822	0.9877	0.98225	0.25
	200–300	0.25	0.459803	0.3709	0.4598	0.37095	0.25
1:4/1:2	300–400	0.25	0.693323	0.5993	0.6933	0.59930	0.25
	400–450	0.25	0.517304	0.3812	0.5173	0.38126	0.25
	450–500	0.25	0.678703	0.5728	0.6787	0.57280	0.25
	23–100	0.0625	0.345734	0.3263	0.3457	0.32638	0.0625
	100–200	0.0625	2.159769	2.2410	2.1597	2.24106	0.0625
1:4/1.0	200–300	0.0625	0.26627	0.2038	0.2662	0.20385	0.0625
	300–400	0.0625	0.280159	0.2135	0.2801	0.21358	0.0625
	400–450	0.0625	0.315988	0.2128	0.3159	0.21280	0.0625
	450–500	0.0625	0.356377	0.2650	0.8726	0.26504	0.0625
	23–100	0.008	0.516392	0.5190	0.5163	0.51902	0.008
	100–200	0.008	1.480349	1.7031	1.4803	1.70318	0.008
1:10/1.0	200–300	0.008	0.304194	0.3206	0.3041	0.32068	0.008
	300–400	0.008	0.490396	0.5193	0.4903	0.51932	0.008
	400–450	0.008	0.317508	0.3489	0.3175	0.34896	0.008
	450–500	0.008	0.313694	0.3457	0.3136	0.34577	0.008
	23–100	0.03199	0.525814	0.5297	0.5258	0.52976	0.0399
	100–200	0.03199	0.676992	0.7465	0.6769	0.7465	0.0319
1:10/1:2	200–300	0.03199	0.525292	0.5835	0.5252	0.58355	0.0319
	300–400	0.03199	1.213605	1.4572	1.2136	1.45720	0.0319
	400–450	0.03199	0.519793	0.6252	0.5197	0.62520	0.0319
	450–500	0.03199	0.597414	0.7472	0.5974	0.74726	0.0319
	23–100	0.12799	1.493611	1.5902	1.4936	1.59024	0.1279
	100–200	0.12799	0.68542	0.7599	0.6854	0.75998	0.1279
1:10/1:4	200–300	0.12799	1.142427	1.5730	1.1424	1.57309	0.1279
	300–400	0.12799	1.750417	2.4315	1.7504	2.43150	0.1279
	400–450	0.12799	1.004811	1.6398	1.0048	1.63981	0.1279
	450–500	0.12799	0.880229	1.3045	0.8802	1.30456	0.1279

For the amount of heat Q, the two cases presented before were considered, namely $Q_{total}[J]$, $Q_{eff}[J]$, and correspondingly the heat flows were $\dot{Q}_{total}[W]$ and $\dot{Q}_{eff}[W]$, respectively.

In Tables 5 and 6, the main quantities were synthesized, which were considered here as measured values, namely, $\left(\Delta t,\ S_{\varsigma},\ S_{\Delta\tau},\ S_{Q_{total}},\ S_{Q_{eff}}\right)$, all of which were determined by rigorous measurements corresponding to the six prototype-model variants.

In Table 6, the values considered to be references were first listed, against which the same values calculated later by the rigorous application of the Model Law were reported (i.e., compared point-by-point) to all applied thermal regimes.

In a similar way, Table 7 summarizes the quantities which were considered as data obtained by direct measurements corresponding to the six prototype-model variants, that is, $\left(\Delta t,\ S_{\varsigma},\ S_{\Delta\tau},\ S_{\dot{Q}_{total}},\ S_{\dot{Q}_{eff}}\right)$.

Version II resulted in the following values:

Table 7. Version II. Measured values.

		Measured Values			
Model/Prototype	**Tmin–Tmax** Δt [°C]	S_{ς} [−]	$S_{\Delta\tau_{total}}$ [−]	$S_{\dot{Q}_{total}}$ [−]	$S_{\dot{Q}_{eff}}$ [−]
	23–100	2	0.677419	0.98208	0.979727
	100–200	2	0.37037	2.186656	2.281555
1:2/1.0	200–300	2	0.576923	0.579094	0.549528
	300–400	2	1.05	0.404082	0.356384
	400–450	2	0.769231	0.610836	0.558164
	450–500	2	0.777778	0.525086	0.462721
	23–100	2	1.809524	0.352042	0.333138
	100–200	2	0.55	0.987704	0.982251
	200–300	2	3.333333	0.459803	0.370959
1:4/1:2	300–400	2	1.428571	0.693323	0.599302
	400–450	2	6	0.517304	0.381264
	450–500	2	0.785714	0.678703	0.572806
	23–100	4	1.225806	0.345734	0.326384
	100–200	4	0.203704	2.159769	2.24106
1:4/1.0	200–300	4	1.923077	0.26627	0.203852
	300–400	4	1.5	0.280159	0.213582
	400–450	4	4.615385	0.315988	0.212808
	450–500	4	0.611111	0.356377	0.265049
	23–100	10.71479	1.080645	0.516392	0.519029
	100–200	10.71479	0.430556	1.480349	1.703182
1:10/1.0	200–300	10.71479	2.092308	0.304194	0.32068
	300–400	10.71479	1.605	0.490396	0.519326
	400–450	10.71479	1.7	0.317508	0.348966
	450–500	10.71479	0.638889	0.313694	0.345774
	23–100	5.357394	1.595238	0.525814	0.529769
	100–200	5.357394	1.1625	0.676992	0.7465
1:10/1:2	200–300	5.357394	3.626667	0.525292	0.583555
	300–400	5.357394	1.528571	1.213605	1.457208
	400–450	5.357394	2.21	0.519793	0.625203
	450–500	5.357394	0.821429	0.597414	0.747262
	23–100	2.678697	0.881579	1.493611	1.590241
	100–200	2.678697	2.113636	0.68542	0.759989
1:10/1:4	200–300	2.678697	1.088	1.142427	1.573096
	300–400	2.678697	1.07	1.750417	2.431507
	400–450	2.678697	0.368333	1.004811	1.639818
	450–500	2.678697	1.045455	0.880229	1.304563

In Table 8, the values considered to be references were first entered, compared to which the same values were later calculated through the rigorous application of the Model Law. They were compared point-by-point in the case of all applied thermal regimes. The small number of errors was more than likely due to the human factor, which, after a significant number of hours of monitoring the equipment, also showed signs of fatigue, i.e., a decrease in attention. A future automation of the current procurement system would be able to eliminate this shortcoming. However, it must be emphasized that this minimal set of insignificant errors (in number and value) does not compromise the validation process of the Model Law.

Table 8. Version II. Computed values.

	Reference Values (Values for Validation)			Calculated Values with the Model Law		
Model/Prototype	$S_{A_{tr}}$ [−]	$S_{Q_{total}}$ [−]	$S_{Q_{eff}}$ [−]	$S_{Q_{total}}$ [−]	$S_{Q_{eff}}$ [−]	$S_{A_{tr}}$ [−]
	0.25	0.66528	0.663686	0.66528	0.663686	0.25
	0.25	0.809873	0.84502	0.809873	0.84502	0.25
1:2/1.0	0.25	0.334093	0.317035	0.334093	0.317035	0.25
	0.25	0.424286	0.374203	0.424286	0.374203	0.25
	0.25	0.469873	0.429357	0.469873	0.429357	0.25
	0.25	0.4084	0.359894	0.4084	0.359894	0.25
	0.25	0.636907	1.449594	0.637029	0.602821	0.25
	0.25	0.543237	0.540238	0.543237	0.540238	0.25
	0.25	1.532678	1.236531	1.532678	1.236531	0.25
1:4/1:2	0.25	0.990462	0.856146	0.990462	0.856146	0.25
	0.25	3.103827	2.287582	3.103827	2.287582	0.25
	0.25	0.533267	0.450062	0.533267	0.450062	0.25
	0.0625	0.423721	0.400084	0.423803	0.400084	0.0625
	0.0625	0.439953	0.456512	0.439953	0.456512	0.0625
1:4/1.0	0.0625	0.512057	0.392024	0.512057	0.392024	0.0625
	0.0625	0.420239	0.320373	0.420239	0.320373	0.0625
	0.0625	1.458406	0.982188	1.458406	0.982188	0.0625
	0.0625	0.533267	0.161975	0.217786	0.161975	0.0625
	0.008	0.558036	0.560886	0.558036	0.560886	0.008
	0.008	0.637373	0.733314	0.637373	0.733314	0.008
1:10/1.0	0.008	0.636467	0.67096	0.636467	0.67096	0.008
	0.008	0.787085	0.833518	0.787085	0.833518	0.008
	0.008	0.539764	0.593241	0.539764	0.593241	0.008
	0.008	0.200415	0.220911	0.200415	0.220911	0.008
	0.031999	0.838799	0.845108	0.838799	0.845108	0.031998
	0.031999	0.787004	0.867807	0.787004	0.867807	0.031999
1:10/1:2	0.031999	1.905058	2.116358	1.905058	2.116358	0.031999
	0.031999	1.855082	2.227447	1.855082	2.227447	0.031999
	0.031999	1.148743	1.381698	1.148743	1.381698	0.031999
	0.031999	0.490733	0.613822	0.490733	0.613822	0.031999
	0.127994	1.316736	1.401923	1.316736	1.401923	0.127994
	0.127994	1.448729	1.606341	1.448729	1.606341	0.127994
1:10/1:4	0.127994	1.24296	1.711529	1.24296	1.711529	0.127994
	0.127994	1.872946	2.601712	1.872946	2.601712	0.127994
	0.127994	0.370105	0.604	0.370105	0.604	0.127994
	0.127994	0.920239	1.363862	0.920239	1.363862	0.127994

4. Final Remarks

Considering the presented results, the following conclusions could be drawn:

- With the data obtained in reference [40], for the two significant versions I and II, the validation calculations of the significant elements of the *ML* were performed;
- *MDA* presented a series of facilities, regarding its simplification, and were deduced for the general case and analyzed in detail in the Introduction section;
- In this sense, it is also worth highlighting those related to ignoring some scale factors in the event of:
  - i. existing implicit correlations (for example: the same type of material existing in the prototype and in the model, or there being identical environmental and deployment conditions for the experimental investigations in the prototype and in the model);
  - ii. existing over-definition of the parameters (such as, for example, accepting the same scale of all lengths $S_{L_x} = S_{L_y} = S_{L_z} = const.$ when the scales and scale factors of the areas no longer have a purpose, so they can be neglected from the above-mentioned analysis);

- With the help of the variables ($\delta_{y\ steel}$,$\delta_{z\ steel}$), it became possible to design models even with different wall thicknesses along the two coordinates $(y\ ,\ z)$, i.e., to ensure models with different areas, obviously; with strict compliance to the scales of these variables imposed by the related elements of the *ML*, the obligation of the existence of a geometric similarity of the cross-sections (prototype-model) can be eliminated;
- The case of the quadratic section was an obvious particular case of the rectangular one;
- The advantage of the simultaneous inclusion of both length (L_z) and shape factor (ς) in the set of independent variables ensured the definition of more general models; where the preservation of geometric similarity is not mandatory, the model can also have a different cross-sectional shape, only to provide a certain scale factor for (ς);
- Inclusion of $(\lambda_{x\ steel})$ among the elements of the A matrix also provides us with the opportunity (if needed) to choose another material for the model in order to reduce the cost price of making and/or testing the model;
- Considering (Q) or $\left(\dot{Q}\right)$ as independent variables also ensures a great freedom in choosing the thermal-stress strategy of the model compared with that of the prototype;
- Inclusion of (Δt) in the set of independent variables provides the researcher the opportunity to choose a thermal regime as favorable as possible for loading the model in relation to the prototype;
- Considering the time of exposure (τ) to a certain thermal regime in the set of independent variables provides another benefit of the use/application of *MDA* to follow the thermal transfer to structures subject to fires.

5. Conclusions

The particular cases mentioned come to illustrate/underline the net advantages of *MDA*. *MDA* can become a useful tool for researchers in the evaluation and simulation of thermal transfer phenomena and last but not least in the analysis of the complex phenomenon of fires in metal-resistance structures. The *M*L, deduced for straight bars, can also be applied to structural elements formed by straight bars, having the same cross-sections, which is obviously found in all civil and industrial structures. Consequently, these laws can also be extended to structural elements, which are realized at various scales, allowing the realization of very convenient models from the point of view of experimental simulations for complex structures (for example, industrial halls with several compartments and respective floors having one or more fire outbreaks arranged as desired). The measurement data obtained on these models, i.e., their responses to fires, will serve, through the application of these *ML*, to optimize real structures subjected to similar fires. The data presented/synthesized in Tables 4 and 5 showed that identical practical values of the quantities were obtained from direct measurements with those expected by the *ML*, thus resulting in the validation of these laws offered by the *MDA*.

Since *ML* was also validated on the 1:10-scale model, it can be stated that it can also be applied to other models, made at convenient scales, to be attached to the prototype. It can be stated that it (*ML*) remains valid for virtually any model made at a desired scale and thus represents a generally valid link between a prototype and a model made at a convenient reduced scale.

Taking into account the facilities and flexibility of the *MDA*, it can be stated that, in the future, the models attached to the prototype may have/present not only different geometric shapes, but also be subject to thermal regimes favorable to the simplest possible experimental investigations, while at the same time being safe, so that the usual (common) researchers can apply it in the analysis of thermal transfer phenomena and through this also obtain information especially useful for those in the field of the fire protection of structures;

The application of this *ML* to complex structural elements, but also to building models, thus becomes a certainty, and the cost price of some investigations (on models made at a convenient scale) becomes particularly advantageous to all those interested in this very important field of constructions, both civil and industrial.

As a significant contribution of the authors, the validity of some rigorous correlations, provided by the Model Law, between the amounts of heat, the thermal flows introduced into the two structures, and also between their geometric elements (areas, dimensions, etc.) represented a natural scale, respectively a scale of up to 1:10. Thus, the modeling of fire scenarios is possible with particularly simple and cheap equipment with the involvement of a minimum number of specialists, and with a rigorously controllable reproducibility of the heating process (of simulating fires).

The purpose of future research by the authors will be precisely these last major aspects of fire protection in buildings.

Author Contributions: Writing—original draft preparation R.-I.S., I.S., S.V., P.-B.G., K.J., T.G., G.P. and Z.A.; writing—review and editing, R.-I.S., I.S., S.V., P.-B.G., K.J., T.G., G.P. and Z.A.; visualization; supervision; project administration; and funding acquisition, R.-I.S., I.S., S.V., P.-B.G., K.J., T.G., G.P. and Z.A. All authors have read and agreed to the published version of the manuscript.

Funding: This research received no external funding. The APC was funded by Transilvania University of Brasov.

Institutional Review Board Statement: Not applicable.

Informed Consent Statement: Not applicable.

Data Availability Statement: Not applicable.

Conflicts of Interest: The authors declare no conflict of interest.

References

1. Munteanu (Száva), I.R. Investigation Concerning Temperature Field Propagation along Reduced Scale Modelled Metal Structures. Ph.D. Thesis, Transilvania University of Brasov, Brașov, Romania, 2018.
2. Al-Homoud, M.S. Performance characteristics and practical applications of common building thermal insulation materials. *Build. Environ.* **2005**, *40*, 353–366. [CrossRef]
3. Bailey, C. Indicative fire tests to investigate the behaviour of cellular beams protected with intumescent coatings. *Fire Saf. J.* **2004**, *39*, 689–709. [CrossRef]
4. Khan, M.A.; Irfan, S.; Rizvi, Z.; Ahmad, J. A numerical study on the validation of thermal formulations towards the behaviour of RC beams. *Mater. Today Proc.* **2019**, *17*, 227–234. [CrossRef]
5. Lawson, R. Fire engineering design of steel and composite buildings. *J. Constr. Steel Res.* **2001**, *57*, 1233–1247. [CrossRef]
6. Noack, J.; Rolfes, R.; Tessmer, J. New layerwise theories and finite elements for efficient thermal analysis of hybrid structures. *Comput. Struct.* **2003**, *81*, 2525–2538. [CrossRef]
7. Papadopoulos, A. State of the art in thermal insulation materials and aims for future developments. *Energy Build.* **2005**, *37*, 77–86. [CrossRef]
8. Quintier, G.J. *Fundamentals of Fire Phenomena*; John Willey & Sons: Hoboken, NJ, USA, 2006.
9. Tafreshi, A.; Marzo, M. Foams and gels as fire protection agents. *Fire Saf. J.* **1999**, *33*, 295–305. [CrossRef]
10. Wong, M.; Ghojel, J. Sensitivity analysis of heat transfer formulations for insulated structural steel components. *Fire Saf. J.* **2003**, *38*, 187–201. [CrossRef]
11. Yang, K.-C.; Chen, S.-J.; Lin, C.-C.; Lee, H.-H. Experimental study on local buckling of fire-resisting steel columns under fire load. *J. Constr. Steel Res.* **2005**, *61*, 553–565. [CrossRef]
12. Guo, Z.; Wang, Y.; Lu, N.; Zhang, H.; Zhu, F. Behaviour of a two-pinned steel arch at elevated temperatures. *Thin-Walled Struct.* **2016**, *107*, 248–256. [CrossRef]
13. Choe, L.; Zhang, C.; Luecke, W.E.; Gross, J.L.; Varma, A.H. Influence of Material Models on Predicting the Fire Behavior of Steel Columns. *Fire Technol.* **2016**, *53*, 375–400. [CrossRef]
14. Ahn, H.J.; An, J.H.; Yeo, I.H.; Hwang, K.J. The relationship between temperature behaviors and section factors of fire spray protection coated composite beams exposed to standard fire. *Int. J. Steel Struct.* **2015**, *15*, 853–861. [CrossRef]
15. Zhang, C.; Silva, J.G.; Weinschenk, C.G.; Kamikawa, D.; Hasemi, Y. Simulation Methodology for Coupled Fire-Structure Analysis: Modeling Localized Fire Tests on a Steel Column. *Fire Technol.* **2016**, *52*, 239–262. [CrossRef]
16. Bączkiewicz, J.; Malaska, M.; Pajunen, S.; Heinisuo, M. Experimental and numerical study on temperature distribution of square hollow section joints. *J. Constr. Steel Res.* **2018**, *142*, 31–43. [CrossRef]
17. He, S.-B.; Shao, Y.-B.; Zhang, H.-Y.; Yang, D.-P.; Long, F.-L. Experimental study on circular hollow section (CHS) tubular K-joints at elevated temperature. *Eng. Fail. Anal.* **2013**, *34*, 204–216. [CrossRef]
18. He, S.; Shao, Y.; Zhang, H.; Wang, Q. Parametric study on performance of circular tubular K-joints at elevated temperature. *Fire Saf. J.* **2015**, *71*, 174–186. [CrossRef]

19. He, S.; Shao, Y.; Zhang, H. Evaluation on fire resistance of tubular K-joints based on critical temperature method. *J. Constr. Steel Res.* **2015**, *115*, 398–406. [CrossRef]
20. Gao, F.; Guan, X.-Q.; Zhu, H.-P.; Liu, X.-N. Fire resistance behaviour of tubular T-joints reinforced with collar plates. *J. Constr. Steel Res.* **2015**, *115*, 106–120. [CrossRef]
21. Kado, B.; Mohammad, S.; Lee, Y.H.; Shek, P.N.; Kadir, M.A. Ab Temperature Analysis of Steel Hollow Column Exposed to Standard Fire. *J. Struct. Technol.* **2018**, *3*, 1–8.
22. Ferraz, G.; Santiago, A.; Rodrigues, J.P.; Barata, P. Thermal Analysis of Hollow Steel Columns Exposed to Localised Fires. *Fire Technol.* **2016**, *52*, 663–681. [CrossRef]
23. Franssen, J.-M. Calculation of temperature in fire-exposed bare steel structures: Comparison between ENV 1993-1-2 and EN 1993-1-2. *Fire Saf. J.* **2006**, *41*, 139–143. [CrossRef]
24. Ghojel, J.; Wong, M. Heat transfer model for unprotected steel members in a standard compartment fire with participating medium. *J. Constr. Steel Res.* **2005**, *61*, 825–833. [CrossRef]
25. Carabogdan, G.I.; Badea, A.; Brătianu, C.; Muşatescu, V. *Methods of Analysis of Thermal Energy Processes and Systems*; Technical Publishing House: Bucharest, Romania, 1989.
26. Barenblatt, G.I. *Dimensional Analysis*; Gordon and Breach: New York, NY, USA, 1987.
27. Carlson, D.E. Some New Results in Dimensional Analysis. *Arch. Ration. Mech. Anal.* **1978**, *68*, 191–210. [CrossRef]
28. Chen, W.-K. Algebraic theory of dimensional analysis. *J. Frankl. Inst.* **1971**, *292*, 403–422. [CrossRef]
29. Coyle, R.G.; Ballico-Lay, B. Concepts and software for dimensional analysis in modeling. *IEEE Trans. Syst. Man, Cybern.* **1984**, *SMC-14*, 478–482. [CrossRef]
30. Gibbings, J.C. Dimensional Analysis. *J. Phys. A-Math. Gen.* **1980**, *13*, 75–89. [CrossRef]
31. Martins, R.D.A. The origin of dimensional analysis. *J. Frankl. Inst.* **1981**, *311*, 331–337. [CrossRef]
32. El Nakla, M. On fluid-to-fluid modeling of film boiling heat transfer using dimensional analysis. *Int. J. Multiph. Flow* **2011**, *37*, 229–234. [CrossRef]
33. Nezhad, A.H.; Shamsoddini, R. Numerical three-dimensional analysis of the mechanism of flow and heat transfer in a vortex tube. *Therm. Sci.* **2009**, *13*, 183–196. [CrossRef]
34. Pankhurst, R.C. *Dimensional Analysis and Scale Factor*; Chapman & Hall Ltd.: London, UK, 1964.
35. Remillard, W.J. Applying dimensional analysis. *Am. J. Phys.* **1983**, *51*, 137–140. [CrossRef]
36. Romberg, G. Beitrag zur Dimensionsanalyse. *Ingenieur-Archiv* **1985**, *55*, 401–412. [CrossRef]
37. Schnittger, J.R. Dimensional Analysis in Design. *J. Vib. Acoust.* **1988**, *110*, 401–407. [CrossRef]
38. Szekeres, P. The mathematical foundations of dimensional analysis and the question of fundamental units. *Int. J. Theor. Phys.* **1978**, *17*, 957–974. [CrossRef]
39. Száva, I.R.; Șova, D.; Dani, P.; Élesztős, P.; Száva, I.; Vlase, S. Experimental Validation of Model Heat Transfer in Rectangular Hole Beams Using Modern Dimensional Analysis. *Mathematics* **2022**, *10*, 409. [CrossRef]
40. Sova, D.; Száva, I.R.; Jármai, K.; Száva, I.; Vlase, S. Heat transfer analysis in a beam with rectangular-hole using Modern Dimensional Analysis. *Mathematics* **2022**, *10*, 409.
41. Szirtes, T. The Fine Art of Modelling. *SPAR J. Eng. Technol.* **1992**, *1*, 37.
42. Szirtes, T. *Applied Dimensional Analysis and Modelling*; McGraw-Hill: Toronto, ON, Canada, 1998.
43. Száva, I.; Szirtes, T.; Dani, P. An Application of Dimensional Model Theory in The Determination of the Deformation of a Structure. *Eng. Mech.* **2006**, *13*, 31–39.
44. Dani, P.; Száva, I.R.; Kiss, I.; Száva, I.; Popa, G. Principle schema of an original full-, and reduced-scale testing bench, destined to fire protection investigations. *Ann. Fac. Eng. Hunedoara-Int. J. Eng.* **2018**, *16*, 149–152.
45. Turzó, G.; Száva, I.R.; Gálfi, B.-P.; Száva, I.; Vlase, S.; Hoța, H. Temperature distribution of the straight bar, fixed into a heated plane surface. *Fire Mater.* **2018**, *42*, 202–212. [CrossRef]
46. Trif, I.; Asztalos, Z.; Kiss, I.; Élesztős, P.; Száva, I.; Popa, G. Implementation of the Modern Dimensional Analysis in Engineering Problems; Basic Theoretical Layouts. *Ann. Fac. Eng. Hunedoara* **2019**, *17*, 73–76.